Coexistence of tetrahedral- and octahedral-like sites in amorphous phase change materials

S. Caravati and M. Bernasconi[a]

Dipartimento di Scienza dei Materiali, Università di Milano-Bicocca, Via R. Cozzi 53, I-20125 Milano, Italy

T. D. Kühne, M. Krack, and M. Parrinello

Computational Science, Department of Chemistry and Applied Biosciences, ETH Zurich, USI Campus, Via Giuseppe Buffi 13, 6900 Lugano, Switzerland

Chalcogenide alloys are materials of interest for optical recording and nonvolatile memories. We perform *ab initio* molecular dynamics simulations aiming at shading light onto the structure of amorphous $Ge_2Sb_2Te_5$ (GST), the prototypical material in this class. First principles simulations show that amorphous GST obtained by quenching from the liquid phase displays two types of short range order. One third of Ge atoms are in a tetrahedral environment while the remaining Ge, Sb, and Te atoms display a defective octahedral environment, reminiscent of cubic crystalline GST. © *2007 American Institute of Physics*. [DOI: 10.1063/1.2801626]

Phase change materials based on chalcogenide alloys are presently used in digital versatile disk (DVD) and are promising materials for nonvolatile electronic memories.[1] Both applications rely on the reversible and fast transition between the amorphous and crystalline phases which have different optical and electronic properties. Among the chalcogenide glasses, $Ge_2Sb_2Te_5$ (GST) is the material of choice for nonvolatile memory applications due to its superior performances in terms of speed of transformation and stability of the amorphous phase.[1]

In spite of its great technological importance, the microscopic structures of amorphous GST (*a*-GST) and the detailed mechanism of the phase transformation are largely unknown.[2] In the past, the structure of *a*-GST was implicitly assumed to be a disordered version of the metastable cubic (rocksalt) crystalline geometry. Very recently, based on extended x-ray absorption fine structure (EXAFS) x-ray absorption near-edge structure (XANES) measurements, Kolobov *et al.*[3] proposed that in *a*-GST, Ge is tetrahedrally coordinated as opposed to its octahedral coordination in the crystalline phases (hexagonal and metastable cubic). Based on *ab initio* calculations, Wełnic *et al.*[4] proposed a spinel-like geometry for the local structure of *a*-GST. However, the model of *a*-GST proposed by Kolobov *et al.* is in contrast with other interpretation of EXAFS data,[5] and with more recent reverse Monte-Carlo (RMC) models fitted to x-ray diffraction (XRD) data.[6] On the other hand, models produced by RMC are subject to large uncertainties when fitted to the total scattering function only, which for *a*-GST is the weighted sum of six partial pair correlation functions. Further investigations are required to obtain a more compelling characterization of *a*-GST, which would facilitate the search for better performing materials.

In this respect, first principles atomistic simulations can provide precious insight. On the basis of successful previous studies on the crystalline phases,[4,7,8] it is to be expected that the density functional theory works well also for the amorphous GST investigated here.

Ab initio molecular dynamics simulations have been performed using the scheme of Kühne *et al.*[9] In the spirit of the Car-Parrinello (CP) approach, the wavefunction is not self-consistently optimized during the dynamics. However, in contrast to CP, large integration time steps can be used in the simulation. This scheme leads to a slightly dissipative dynamics of the type $-\gamma_D \dot{\mathbf{R}}_I$, where $\mathbf{R}_I$ are the ionic coordinates. In Ref. 9, it is shown how to compensate for this dissipation and obtain a correct canonical sampling. This scheme has been implemented in the CP2K suite of programs.[10,11] We use a gradient corrected exchange correlation functional[12] and Goedecker-type pseudopotentials.[13] The
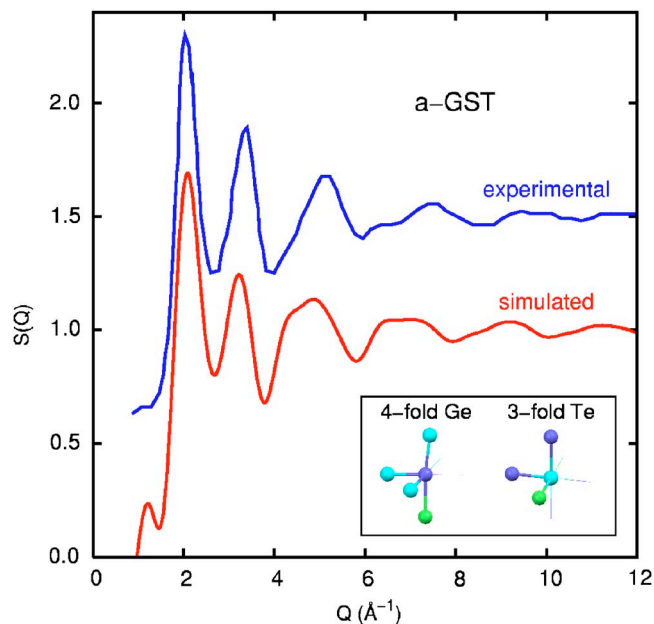

FIG. 1. (Color online) Calculated and experimental (Ref. 6) x-ray scattering factor $S(Q)$ of *a*-GST. The theoretical $S(Q)$ has been computed from the partial structure factors $S_{ij}(Q)$ weighted by the Q-dependent x-ray atomic form factors (Ref. 22) [$S(Q)-1=F^X(Q)$] of Eq. (56) in Ref. 23]. $S_{ij}(Q)$ are obtained in turn by Fourier transforming the partial pair correlation functions (3 ps at 300 K). Inset: a sketch of the geometry of defective octahedral sites of four-coordinated Ge and three-coordinated Te.

---
[a]Electronic mail: marco.bernasconi@mater.unimib.it

TABLE I. Average coordination number for different pairs of atoms computed from the partial pair correlation functions [Fig. S4 in EPAPS (Ref. 16)].

	Average coordination number			
	With Ge	With Sb	With Te	Total
Ge	0.275	0.270	3.277	3.823
Sb	0.270	0.588	3.166	4.025
Te	1.311	1.267	0.288	2.866

Kohn-Sham orbitals are expanded in a valence triple-zeta plus polarization (TZVP) Gaussian-type basis set, and the charge density is expanded in a planewave basis set with a cutoff of 100 Ry.

The initial configuration is the metastable cubic GST, where Te occupies one sublattice of the rocksalt crystal, and Ge, Sb, and vacancies are randomly placed in the other sublattice in an orthorhombic supercell of size $21.97 \times 21.97 \times 18.63$ Å^3 (270 atoms) at the density of 0.030 at./Å^3 close to the experimental value for a-GST.[14] The system has then been heated and equilibrated for 6 ps at 2300 K and then quenched in 16 ps and further equilibrated for 18 ps at 990 K. The parameter $\gamma_D = 4 \times 10^{-4}$ fs^{-1} has been determined as in Ref. 9. The static properties of liquid GST turned out to be in good agreement with the experiments[6,15] as detailed in the supplementary materials [Figs. S1–S3 in EPAPS (Ref. 16)]. In order to generate a model of a-GST, the liquid has been brought to 300 K in 18 ps. The calculated x-ray scattering function $S(Q)$ of a-GST reported in Fig. 1 is in good agreement with the XRD data,[6] especially considering that the latter are on the as-deposited amorphous film which might be structurally slightly different from a-GST quenched from the melt as suggested by their different optical reflectivity.[17] Incidentally, we recall that a-GST of relevance for applications is the phase quenched from the melt for which no XRD data are available. Average coordination numbers for the different species of a-GST (Table I) are computed from partial pair correlation functions [Fig. S4 in EPAPS (Ref. 16)]. The distribution of the coordination number for the different species are reported in the inset of Fig. 2. Ge and Sb atoms are mostly four-coordinated and form
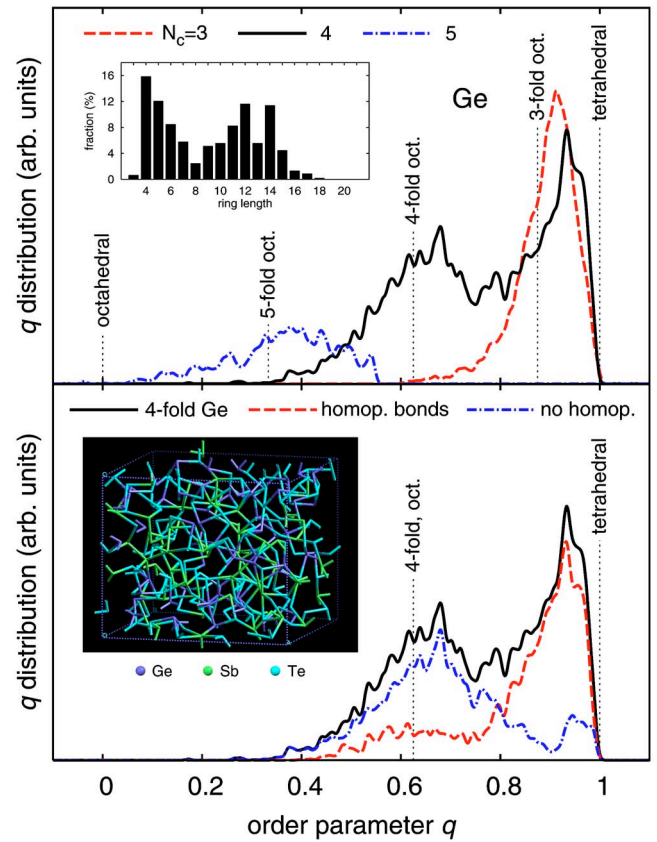
FIG. 3. (Color online) Distribution of the local order parameter q for Ge with different coordination numbers (N_c) (see text). $q=1$ for the ideal tetrahedral geometry, $q=0$ for the six-coordinated octahedral site, and $q=5/8$ for a four-coordinated defective octahedral site. Top panel: q-distribution resolved for Ge with different coordination number. Bottom panel: q-distribution for four-coordinated Ge further resolved for Ge with at least one homopolar bond (with Ge or Sb) or bonding with Te only (no homopolar bonds). Top panel inset: ring distribution function of a-GST computed as in Ref. 20. Bottom panel inset: snapshot of the 270-atom model of a-GST.

bonds preferentially with Te atoms. However, we observe a large fraction of homopolar Ge–Ge, Sb–Sb and Ge–Sb bonds, namely, 38% of Ge are bonded with at least another Ge or Sb, a percentage which is raised to 52% for Ge atoms four-coordinated. The fraction of Sb bonded to another Sb or Ge is instead 59%. Homopolar Ge–Ge bonds have been recently detected by x-ray fluorescence in cubic GST grown epitaxially on crystalline GaSb.[18] The concentration of Te–Te bonds is somehow lower; 27% of Te atoms are involved in homopolar Te–Te bonds arranged into dimers and trimers [see Fig. S5 in EPAPS (Ref. 16)]. The large concentration of homopolar bonds is not reproduced by the RMC model.[6] Insight on the local geometry is further gained from the angle distribution function in Fig. 2. The broad peak at $\sim 90°$ and the weaker structure around $\sim 170°$ are reminiscent of the distorted octahedral-like geometry of the metastable cubic crystal. A snapshot of the a-GST model is shown in Fig. 3. Angles at $\sim 90°$ and $\sim 180°$ clearly dominate the bonding network. However, the main coordination of Ge(Sb) and Te of four and three, respectively, is lower than the ideal octahedral value of six. In our model, the presence of neighboring vacancies is responsible for the lower coordination, while the bonding angles remain close to $\sim 90°$ and $\sim 180°$ as in the metastable cubic phase. For three-coordinated Te, only angles at $\sim 90°$ are found (see inset of Fig. 1). Te and Sb atoms adopt this configuration, while only a fraction of Ge
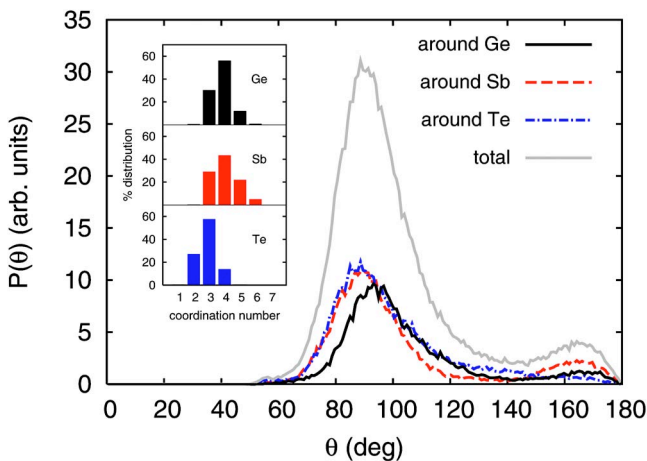

FIG. 2. (Color online) Angle distribution function (total and resolved for different central atoms). Inset: distribution of coordination numbers of different species obtained by integration of the partial pair correlation functions [Fig. S4 in EPAPS (Ref. 16)].

atoms are in a defective octahedral site. A large fraction of four-coordinated Ge atoms are in a tetrahedral environment as inferred from EXAFS/XANES measurements.[3] A signature of the tetrahedral geometry is already visible as a shoulder at ∼110° in the angle distribution function for Ge atoms in Fig. 2. A better indicator of the tetrahedral geometry is given by the local order parameter[19] $q = 1 - \frac{3}{8}\sum_{i>k}(\frac{1}{3} + \cos\theta_{ijk})^2$, where the sum runs over the couples of atoms bonded to a central atom j. The distribution of the local order parameter q for Ge atoms is reported in Fig. 3 for different coordination numbers. The four-coordinated Ge distribution is clearly bimodal with peaks corresponding to defective octahedra and tetrahedra. In contrast, the q-distribution for Te and Sb does not show any signature of the tetrahedral geometry [Fig. S6 in EPAPS (Ref. 16)]. The q-distribution for four-coordinated Ge is further analyzed in terms of atoms bonded to Te only or to at least one Ge or Sb. The presence of bonds with Ge or Sb clearly favors the tetrahedral geometry. Only few tetrahedral Ge are bonded to Te only. On the other hand, all Ge with more than one homopolar bond (with Ge or Sb) are in the tetrahedral geometry. By integrating the tetrahedral peak of the q-distribution in the range of 0.8-1.0, we estimate that 33% of Ge atoms are in a tetrahedral environment. The average bond length of Ge is slightly shorter in tetrahedral sites (2.73 Å) than in defective octahedral sites [2.82 Å, see Fig. S6 in EPAPS (Ref. 16)]. The presence of tetrahedral sites and the absence of six-coordinated octahedral sites [or distorted octahedra sites with 3+3 coordination as in crystalline α-GeTe (Ref. 21)] is consistent with the model inferred from EXAFS/XANES data in Ref. 3. The coexistence of tetrahedral and defective octahedral sites found here might reconcile the different interpretation of EXAFS data[3,5] based on the assumption of a unique environment for all Ge atoms. The inclusion of both configurations in a revised fitting might provide a better agreement with the experiments. Turning now to the medium range order of a-GST, we report the ring distribution in Fig. 3. Both even and odd rings are present, as opposed to the RMC results.[6] The distribution has a pronounced maximum at four-membered rings typical of the rocksalt structure. 82% of four-membered rings are in the form $ABAB$, without homopolar bonds. The presence of very large rings (with very large aspect ratio) reveals a somehow more open and less connected structure than that of the cubic crystalline phase.

In summary, based on first principles simulations, we have provided insight into the structure of amorphous $Ge_2Sb_2Te_5$ quenched from the melt. Most of the Ge and Sb atoms in a-GST are four-coordinated, while Te is mostly three-coordinated in defective octahedral-like sites which recall the local environment of cubic crystalline GST. However, as many as 33% of Ge atoms are in a tetrahedral geometry, absent in the crystalline phase, and favored by the presence of homopolar (Ge–Ge and Ge–Sb) bonds. The coexistence of the two types of local environment might be the key to understand the two apparently contradictory and peculiar features of GST exploited in the devices, namely, the strong optical (and perhaps electronic) contrast between the amorphous and crystalline structures, and the high speed of the phase change. This conclusion is also supported by the recent theoretical work in Ref. 7 on models of amorphous GeSbTe alloys showing that the presence of a fraction of Ge in tetrahedral sites is indeed sufficient to produce a strong optical contrast between the amorphous and crystalline phases.

[1]A. Pirovano, A. L. Lacaita, A. Benvenuti, F. Pellizzer, and R. Bez, IEEE Trans. Electron Devices **51**, 452 (2004); S. Hudgens and B. Johnson, Mater. Res. Soc. Bull. **29**, 829 (2004); M. Wuttig, Nat. Mater. **4**, 265 (2005).

[2]A. L. Greer and N. Mathur, Nature (London) **437**, 1246 (2005).

[3]A. V. Kolobov, P. Fons, A. I. Frenkel, A. L. Ankudinov, J. Tominaga, and T. Uruga, Nat. Mater. **3**, 703 (2004).

[4]W. Wełnic, A. Pamungkas, R. Detemple, C. Steimer, S. Blügel, and M. Wuttig, Nat. Mater. **5**, 56 (2006).

[5]D. A. Baker, M. A. Paesler, G. Lucovsky, S. C. Agarwal, and P. C. Taylor, Phys. Rev. Lett. **96**, 255501 (2006).

[6]S. Kohara, K. Kato, S. Kimura, H. Tanaka, T. Usuki, K. Suzuya, H. Tanaka, Y. Moritomo, T. Matsunaga, N. Yamada, Y. Tanaka, H. Suematsu, and M. Takata, Appl. Phys. Lett. **89**, 201910 (2006).

[7]W. Wełnic, S. Botti, L. Reining, and M. Wuttig, Phys. Rev. Lett. **98**, 236403 (2007).

[8]M. Wuttig, D. Lüsebrink, D. Wamwangi, W. Wełnic, M. Gilleßen, and R. Dronskowski, Nat. Mater. **6**, 122 (2007).

[9]T. D. Kühne, M. Krack, F. R. Mohamed, and M. Parrinello, Phys. Rev. Lett. **98**, 066401 (2007).

[10]M. Krack and M. Parrinello, in *High Performance Computing in Chemistry*, edited by J. Grotendorst (NIC, Jülich, 2004), Vol. 25, pp. 29–51 http://cp2k.berlios.de.

[11]J. VandeVondele, M. Krack, F. Mohamed, M. Parrinello, T. Chassaing, and J. Hutter, Comput. Phys. Commun. **167**, 103 (2005).

[12]J. P. Perdew, K. Burke, and M. Ernzerhof, Phys. Rev. Lett. **77**, 3865 (1996).

[13]S. Goedecker, M. Teter, and J. Hutter, Phys. Rev. B **54**, 1703 (1996); M. Krack, Theor. Chem. Acc. **114**, 145 (2005).

[14]W. K. Njoroge, H. W. Wöltgens, and M. Wuttig, J. Vac. Sci. Technol. A **20**, 230 (2002).

[15]M. Delheusy, J. Y. Raty, R. Detemple, W. Wełnic, M. Wuttig, and J.-P. Gaspard, Physica B **350**, e1055 (2004).

[16]See EPAPS Document No. E-APPLAB-91-029744 for additional figures on structural properties of liquid and amorphous GST. This document can be reached through direct link in the online article's HTML reference section or via the EPAPS home page (http://www.aip.org/pubserv/epaps.html).

[17]J. Park, M. R. Kim, W. S. Choi, H. Seo, and C. Yeon, Jpn. J. Appl. Phys., Part 1 **38**, 4775 (1999).

[18]S. Hosokawa, T. Ozaki, K. Hayashi, N. Happo, M. Fujiwara, K. Horii, P. Fons, A. V. Kolobov, and J. Tominaga, Appl. Phys. Lett. **90**, 131913 (2007).

[19]J. R. Errington and P. G. Debenedetti, Nature (London) **409**, 318 (2001).

[20]D. S. Franzblau, Phys. Rev. B **44**, 4925 (1991).

[21]J. Goldak, C. S. Barrett, D. Innes, and W. Youdelis, J. Chem. Phys. **44**, 3323 (1966).

[22]D. T. Cromer and J. B. Mann, Acta Crystallogr., Sect. A: Cryst. Phys., Diffr., Theor. Gen. Crystallogr. **24**, 321 (1968).

[23]D. A. Keen, J. Appl. Crystallogr. **34**, 172 (2001).